Available online at www.sciencedirect.com
ScienceDirect
Journal of Crystal Growth 300 (2007) 308–313
JOURNAL OF CRYSTAL GROWTH
www.elsevier.com/locate/jcrysgro

Study on optimal growth conditions of *a*-plane GaN grown on *r*-plane sapphire by metal-organic chemical vapor deposition

T.S. Ko[a], T.C. Wang[a], R.C. Gao[a], H.G. Chen[b], G.S. Huang[a], T.C. Lu[a,*], H.C. Kuo[a], S.C. Wang[a]

[a]*Department of Photonics, Institute of Electro-Optical Engineering, National Chiao Tung University, 1001 Ta Hsueh Road, Hsinchu 30050, Taiwan, ROC*
[b]*Department of Materials Science and Engineering, I-Shou University, Kaohsiung 840, Taiwan, ROC*

Received 15 August 2006; received in revised form 27 December 2006; accepted 28 December 2006
Communicated by R. Bhat
Available online 20 January 2007

Abstract

Non-polar *a*-plane $(1\,1\,\bar{2}\,0)$ GaN thin films were grown on *r*-plane $(1\,\bar{1}\,0\,2)$ sapphire substrates by metal-organic chemical vapor deposition. In order to obtain *a*-plane GaN films with better crystal quality and surface morphology, detailed comparisons between different growth conditions were investigated. The results showed that high-temperature and low-pressure conditions facilitating two-dimensional growth could lead to a fully coalesced *a*-plane GaN layer with a very smooth surface. The best mean roughness of the surface morphology was 10.5 Å. Various thickness values of AlN nucleation layers and the V/III ratios for growth of the *a*-plane GaN bulk were also studied to determine the best condition for obtaining a smooth surface morphology of the *a*-plane GaN layer.

PACS: 81.15.Gh; 73.61.Ey; 61.10.Nz; 68.37.Lp

Keywords: A1. X-ray diffraction; A3. Metal-organic chemical vapor deposition; B1. Nitrides

1. Introduction

GaN-based semiconductors and their heterostructures have recently attracted considerable interest due to their potential for visible or ultraviolet light-emitting diodes (LEDs) [1], laser diodes (LDs) [2] and high-power transistors [3] grown on either *c*-plane (0 0 0 1) sapphire, SiC, or free standing GaN substrates. Unfortunately, epitaxy toward the [0 0 0 1] orientation leads to undesirable spontaneous and piezoelectric polarization effects, which would result in inclined bands and significantly reduce the carrier recombination rate in quantum wells grown on such polar substrates [4,5]. To eliminate such polarization effects, growth along non-polar orientations has been explored for $(1\,0\,\bar{1}\,0)$ *m*-plane GaN on *m*-plane SiC and (1 0 0) $LiAlO_2$ substrates, and $(1\,1\,\bar{2}\,0)$ *a*-plane GaN on $(1\,\bar{1}\,0\,2)$ *r*-plane sapphire [6–8].

Growth of non-polar group-III nitride hexagonal heterostructures could overcome the presence of large built-in electrostatic fields to further improve the quantum efficiency of LEDs. However, the surface morphology of the GaN grown on *r*-plane sapphire was usually quite rough, making device fabrication more difficult. As a result, most groups avoided using *r*-plane sapphire substrates to grow GaN devices. In order to overcome the influence of defects generated due to the lattice mismatch, Chitnis et al. [9] grew *a*-plane LED structure on *r*-plane sapphire by using a GaN layer with a thickness of more than 30 μm. Haskell et al. employed epitaxial lateral overgrowth (ELOG) [10]. Although ELOG method could yield *a*-plane GaN films over *r*-plane sapphire with significantly improved surface morphologies and with reduced dislocation densities, this approach was complicated and consumed time-consuming.

In this study, the optimal growth condition of the *a*-plane GaN layers with pits-free and smooth surface were investigated by modifying growth temperatures, pressures,

*Corresponding author. Tel.: +886 3 5131234; fax: +886 3 5716631.
E-mail address: timtclu@faculty.nctu.edu.tw (T.C. Lu).

0022-0248/$ - see front matter © 2007 Elsevier B.V. All rights reserved.
doi:10.1016/j.jcrysgro.2006.12.046

and V/III ratio. Furthermore, the influences of different thicknesses of AlN as nucleation layers were also considered. Eventually, we obtained a high-quality *a*-plane GaN bulk with a smooth surface capable of fabricating device structures, such as multiple quantum wells and LEDs directly on top of it.

2. Experiments

The experiments were carried out in the low-pressure metal-organic chemical vapor deposition (MOCVD) system. We used low-temperature AlN as nucleation layers instead of traditional GaN layers. The nucleation layer growth temperature and thickness were 600 °C and 30 nm, respectively. The V/III ratio for the nucleation layer is 13,800. In order to obtain suitable growth conditions for *a*-plane GaN films, influence of different pressures (100, 200, and 300 Torr) and temperatures (1020, 1070, and 1120 °C) on growth of 2 μm thick GaN bulks was studied. Trimethylgallium (TMGa), trimethylaluminum (TMAl), and ammonia were used as Ga, Al, and N sources, respectively. Then, we fixed the growth pressure and temperature, which would result in the smoothest surface morphology, and would change different thicknesses of AlN nucleation layers from 30 nm to 15 and 45 nm. In addition, the V/III ratio for growth of the GaN bulk was adjusted from 900 to 600 and 1200, subsequently. The surface morphologies of all samples were characterized by optical microscopy (OM) with × magnification, scanning electronic microscopy (SEM) and atomic force microscopy (AFM). Surface step profiles were evaluated using the surface profiler (Veeco Dektak 6M). The crystalline quality was analyzed by high-resolution reciprocal space mapping (RSM) by using X-ray diffraction around the $(1\,1\,\bar{2}\,0)$ reflection.

3. Results and discussion

First, the optimal growth parameters in growth pressure and temperature, to obtain a good surface morphology of an *a*-plane GaN bulk, were studied. The thickness of the AlN nucleation layer and the V/III ratio for growing *a*-plane GaN bulk were fixed as 30 nm and 900, respectively. In order to make all analyses easy to understand, our results and growth parameters were set into a three-by-three square chart. Fig. 1 shows the typical OM images of *a*-plane GaN with different growth conditions. We found the nucleation island did not coalesce fully, causing a rugged and rough surface when the growth pressures were high and temperatures were low, as shown in Fig. 1(f), (h), and (i). Once the growth temperature was elevated and the pressure was decreased, the nucleation islands gradually coalesced with each other and the remaining pits distributed on the sample surface, as shown in Fig. 1(b)–(e) and (g). Fig. 1(a) manifested smoothest surface morphology without any observable pits when the growth temperature and pressure were set as 1120 °C and 100 Torr, respectively.

The surface profiles of *a*-plane GaN were roughly estimated for different growth conditions by the surface profiler. These results of line profiles along the direction perpendicular to [0 0 0 1] are shown in Fig. 2. Fig. 2(a)–(e) and (g) reveals the rough surfaces of these samples with peak to valley (PV) values of around 70 nm, whereas Fig. 2(f)–(h) shows worse PV values from 200 to 600 nm. These results can be compared with another study by

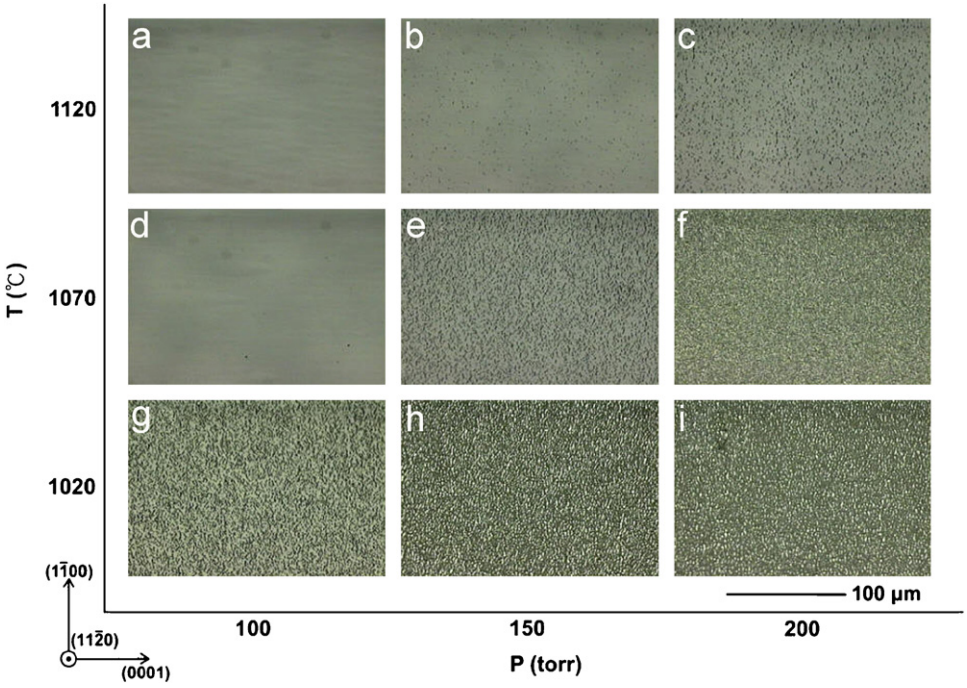

Fig. 1. OM images of *a*-plane GaN surfaces for growth temperatures of 1020–1120 °C and pressures of 100–300 Torr.

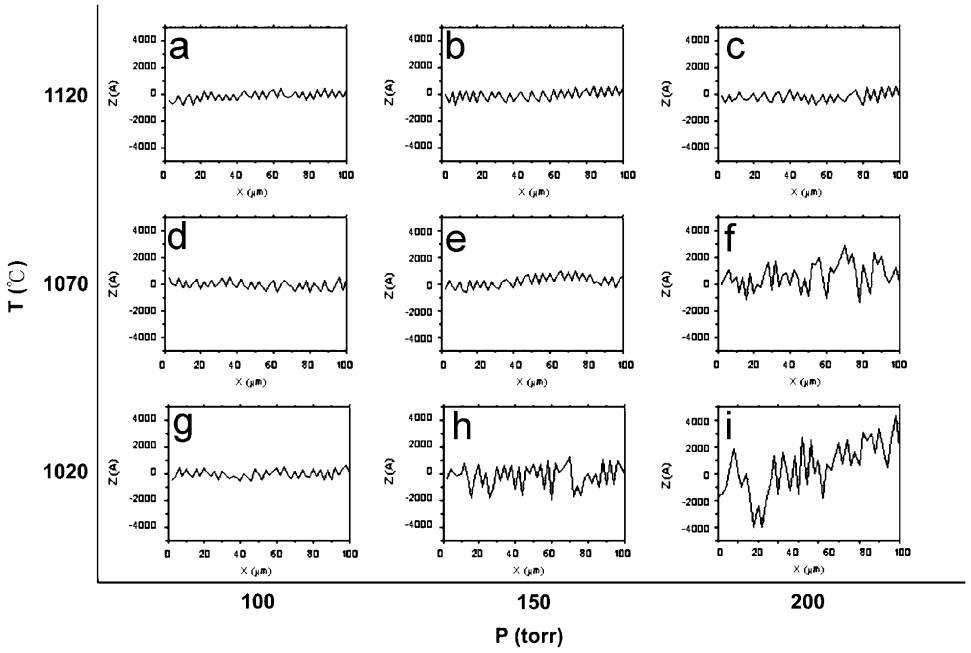

Fig. 2. Surface profiles of *a*-plane GaN epi-layers for growth temperatures of 1020–1120 °C and pressures of 100–300 Torr. *X* is the scan direction along [1 $\bar{1}$ 0 0] and *Z* is the height direction along [1 1 $\bar{2}$ 0].

Kusakabe and Ohkawa [11], who grew *a*-plane GaN in regular growth conditions and obtained a high PV value around 0.8 μm, indicating that the surface profiles were successfully improved in order of magnitude by elevating the growth temperature and diminishing the growth pressure.

The surface morphology images investigated by SEM were enlarged as shown in Fig. 3. The growth condition of high temperature and low pressure resulted in best surface morphology in terms of flatness as shown in Fig. 3(a). However, not only large number of pits existed but also wavy stripes forming along the *c*-axis could be clearly observed in Fig. 3(f), (h), and (i). The possible reason for the strip forming was due to the faster growth rate along *c*-direction than *m*-direction. On the other hand, the irregular strips could not be observed in Fig. 3(b)–(e) and (g) except for triangular pits on the surface. In general, the common feature of V defects is characteristically observed when the *c*-plane GaN is grown in the kinetically limited condition [12]. The V defect for a *c*-plane GaN is an inverted pyramid bound by the pyramidal {1 0 $\bar{1}$ 1} facets. Since the V defect appears only in its half-side in an *a*-plane GaN under the non-polar growth scheme, such kind of pits was named as triangle pit originating from the island growth and coalescing at the initial growth of the high-temperature GaN bulk [13].

As a result, we could suggest that the growth mechanism of *a*-plane GaN at the beginning stage followed a Volmer–Weber (VW) mode, which would lead to the three-dimensional (3D) growth. Each GaN column was probably grown from a GaN island formed on top of AlN nucleation layer. After most of the islands merged each other, a Frank–van der Merwe (F–vdM) mode occurred and dominated the subsequent growth process, leading to two-dimensional (2D) growth. The 2D growth condition is necessary for thick *a*-plane GaN as the difference of growth rate could occur between *c*-axis and *m*-axis. Otherwise, the 3D growth would result in the appearances of triangle pit and wavy strips.

In addition to the effect of epitaxial temperature and pressure, the thickness of the nucleation layer and the V/III ratio for growth of the *a*-plane GaN bulk were also considered. The growth pressure and temperature were fixed to the same values as those resulting in the best surface morphology. Then, the thickness of the nucleation layer and the V/III ratio were modified. The thickness of nucleation layer was adjusted from 30 nm to 15 and 45 nm, and the V/III ratio was adjusted from 900 to 600 and 1200. The surface morphologies of all samples were observed by AFM and the results shown in Fig. 4. The center 3D AFM image is the result of the sample grown at 1120 °C and at 100 Torr, which showed submicro pits and additional stripe features along the [0 0 0 1] direction. Meanwhile, the sample showed a very smooth surface with a root mean square (RMS) roughness of only 10.5 Å. Such roughness was far less than in the previous report by Ni et al., whose sample was grown at lower growth temperature on a thicker nucleation layer [14]. However, when we used AlN nucleation layers with thickness thinner and thicker than 30 nm, the surface morphologies would get worse along with many pits with sizes around 100 nm. Owing to the fact that each GaN column could be grown from GaN nucleus formed on top of each columnar AlN region, the columns of AlN should have optimal disordered orientations for

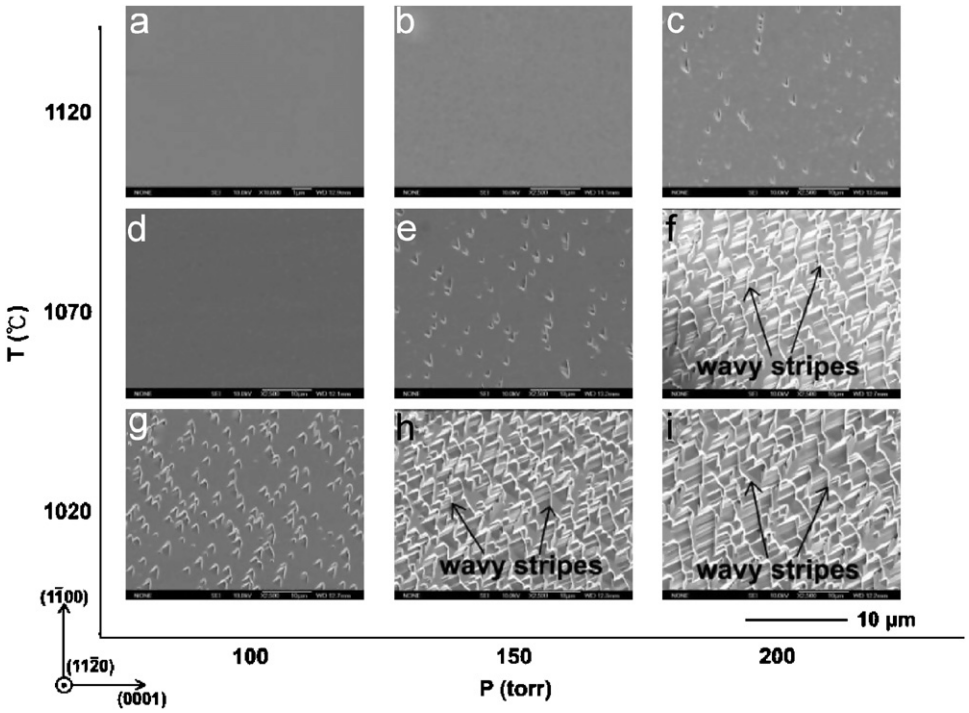

Fig. 3. SEM images of *a*-plane GaN surfaces for growth temperatures of 1020–1120 °C and pressures of 100–300 Torr.

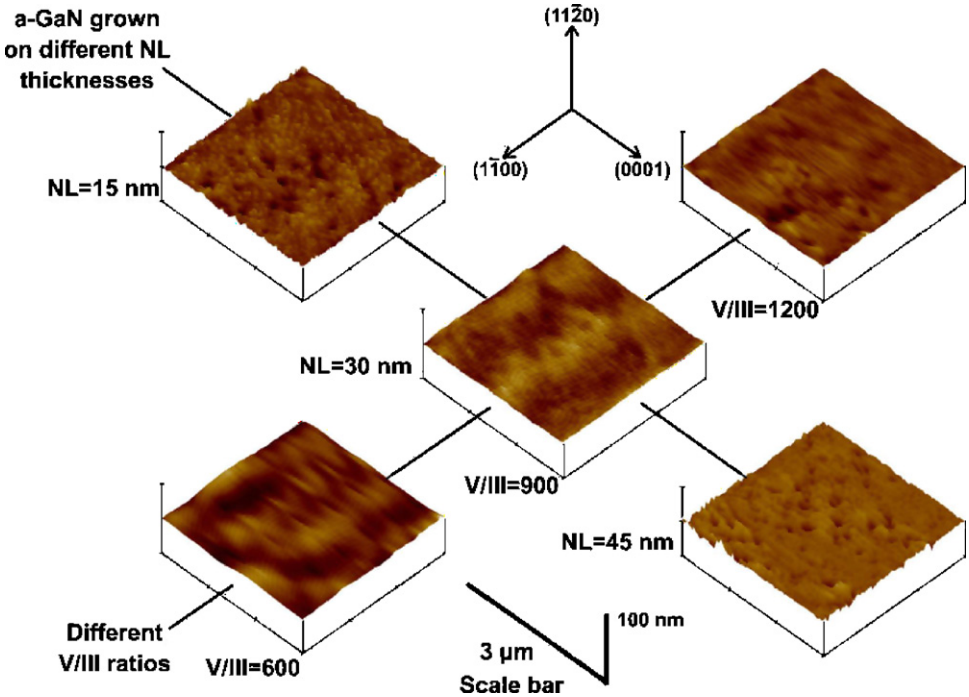

Fig. 4. AFM images of *a*-plane GaN surfaces for growth of V/III ratio of 600–1200 °C and on different thicknesses of AlN nucleation layers.

GaN growth. Once the thickness of AlN nucleation layer has been changed, it could cause the variation of disordered orientations and degrade the surface morphology. On the other hand, the surface morphology got worse when the V/III ratio was increased or decreased from 900. The high V/III ratio led to high NH_3 flow and further produced more amounts of hydrogen during the growth process. Some pits distributed on the surface, under the high V/III ratio, could be due to the excess hydrogen facilitating the surface dissociation rate and damaging the surface morphology [15]. Although the low V/III ratio condition benefits the 2D growth, some Ga atoms would

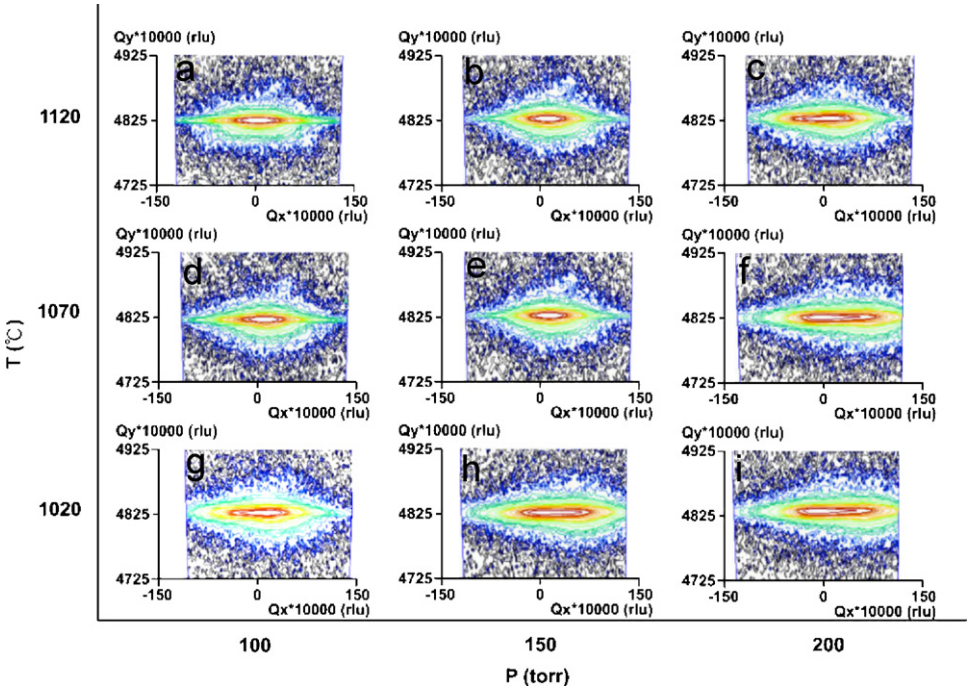

Fig. 5. Reciprocal space mapping of *a*-plane GaN for growth temperatures of 1020–1120 °C and pressures of 100–300 Torr.

not react with insufficient N atoms causing a wavy surface. To sum up the above discussions, we suggest that both the thickness of nucleation layer and the V/III ratio have optimal values to grow an *a*-plane GaN bulk.

X-ray RSMs were recorded around the $(1\,1\,\bar{2}\,0)$ reflection in a coplanar geometry, as shown in Fig. 5. The unit of "r.l.u." refers to dimensionless reciprocal lattice units. The vertical axis in Fig. 5(a) corresponds to the ω-scan around the symmetry $(1\,1\,\bar{2}\,0)$ reflection, and the full-width of height maximum (FWHM) was about 875 arcsec after conversion of the coordinate, demonstrating that the sample grown at high temperature and low pressure could prompt a good-quality GaN film. It is worth noticing that the narrow FWHM of 665 arcsec in ω-scan in Fig. 5(e) under the lower temperature and higher pressure conditions was obtained, although the sample grown by this condition showed several pits in OM and SEM images. This indicates that a more coherent growth condition resulting in a narrower FWHM of ω-scan, did not promise a good surface morphology, which could be due to the different in-plane strains and growth rates along *c*- and *m*-directions. On the other hand, the larger contoured areas shown in Fig. 5(f), (h), and (i) indicated inferior crystal quality due to disordered GaN columns during the growth. As a result, the surface morphology and the crystal quality should be carefully compromised in the growth of *a*-plane GaN films.

4. Conclusion

In conclusion, we grew *a*-plane GaN with a series of growth conditions that included different growth temperatures and chamber pressures by MOCVD. High-quality and smooth-surface *a*-plane GaN could be obtained at high-temperature and low-pressure growth condition. The best mean roughness of the surface morphology was 10.5 Å. Moreover, the thickness of the nucleation layer and V/III ratio for the GaN bulk growth existed in optimal values for obtaining high-quality *a*-plane GaN. Finally, the smooth surface of the *a*-plane GaN film obtained in this study demonstrated the feasibility and convenience of fabricating non-polar devices.

Acknowledgments

This work was supported by the MOE ATU program and in part by the National Science Council of the Republic of China (ROC) in Taiwan under Contract Nos. NSC 95-2120-M-009-008, NSC 95-2752-E-009-007-PAE, and NSC 95-2221-E-009-282.

References

[1] S.J. Pearton, J.C. Zolper, R.J. Shul, F. Ren, J. Appl. Phys. 86 (1999) 1.
[2] S. Nakamura, G. Fasol, in: The Blue Laser Diodes, Springer, Heidelberg, 1997.
[3] T. Palacios, L. Shen, S. Keller, A. Chakraborty, S. Heikman, S.P. DenBaars, U.K. Mishra, J. Liberis, O. Kiprijanovic, A. Matulionis, Appl. Phys. Lett. 89 (2006) 073508.
[4] T. Deguchi, K. Sekiguchi, A. Nakamura, T. Sota, R. Matsuo, S. Chichibu, S. Nakamura, J. Acoust. Soc. Jpn. (E) 38 (1999) L914.
[5] S. Ghosh, P. Waltereit, O. Brandt, H.T. Grahn, K.H. Ploog, Phys. Rev. B 65 (2002) 075202.
[6] K. Domen, K. Horino, A. Kuramata, T. Tanahashi, Appl. Phys. Lett. 71 (1997) 1996.

[7] P. Waltereit, O. Brandt, A. Trampert, H.T. Grahn, J. Menniger, M. Ramsteiner, M. Reiche, K.H. Ploog, Nature 406 (2002) 865.
[8] A. Chitnis, C. Chen, V. Adivarahan, M. Shatalov, E. Kuokstic, V. Mandavilli, J. Yang, M.A. Khan, Appl. Phys. Lett. 84 (2004) 3663.
[9] A. Chitnis, C. Chen, V. Adivarahan, M. Shatalov, E. Kuokstis, V. Mandavilli, J. Yang, M.A. Khan, Appl. Phys. Lett. 84 (2004) 3663.
[10] B.A. Haskell, T.J. Baker, M.B. McLaurin, F. Wu, P.T. Fini, S.P. DenBaars, J.S. Speck, S. Nakamura, Appl. Phys. Lett. 86 (2005) 11917.
[11] K. Kusakabe, K. Ohkawa, Jpn. J. Appl. Phys. 44 (11) (2005) 7931.
[12] X. Wu, C. Elsass, A. Abare, M. Mack, S. Keller, P. Petroff, S. DenBaars, J. Speck, S. Rosner, Appl. Phys. Lett. 72 (1998) 692.
[13] F. Wu, M.D. Craven, S.H. Lim, J.S. Speck, J. Appl. Phys. 94 (2003) 942.
[14] X. Ni, Y. Fu, Y.T. Moon, N. Biyikli, H. Morkoç, J. Crystal Growth 290 (2006) 166.
[15] T.H. Myers, B.L. VanMil, J.J. Holbert, C.Y. Peng, C.D. Stinespring, J. Alam, J.A. Freitas Jr., V.A. Dmitriev, A. Pechnikov, Y. Shapovalova, V. Ivantsov, J. Crystal Growth 246 (2002) 244.